Magnesium Technology 2011
Edited by: Wim H. Sillekens, Sean R. Agnew, Neale R. Neelameggham, and Suveen N. Mathaudhu
TMS (The Minerals, Metals & Materials Society), 2011

EFFECT OF Mn ADDITION ON CREEP PROPERTY IN Mg-2Al-2Ca SYSTEMS

T. Homma[1], S. Nakawaki[1], K. Oh-ishi[2], K. Hono[2], S. Kamado[1]
[1]Department of Mechanical Engineering, Nagaoka University of Technology, Nagaoka 940-2188, Japan
[2]National Institute for Materials Science, 1-2-1 Sengen, Tsukuba 305-0047, Japan

Keywords: Magnesium alloy, Creep, Transmission electron microscopy, Atom probe tomography

Abstract

Planar Al_2Ca phase forms on the basal plane in the as-cast AX22 and AXM220 alloys. In the AXM220 alloy, Mn is detected in the Al_2Ca phase. The number density of the Al_2Ca phase does not alter, irrespective of the creep deformation and Mn addition. Fine and planar precipitates appear during the creep deformation. The number density increases by the addition of Mn. The size of the precipitate is reduced by the Mn addition. The Mn addition can improve the creep property.

Introduction

Rare-earth-containing Mg alloys have widely been investigated since they demonstrate remarkable creep properties [1-6]. The latest papers suggest that the improvement in the creep properties is related to dispersion of fine precipitates [4-6]. However, the addition of the rare-earth element into the Mg alloys is indeed costly. Therefore, the development in new-type of magnesium alloys containing "ubiquitous elements" is required.

Al- and Ca-containing Mg alloys attract a lot of attention due to their cost performance and high temperature properties [7-12]. In particular, the use of the materials is expected in automobile industries [13-15]. The advantage in utilizing the Mg-Al-Ca-based alloys is due to the formation of $(Mg,Al)_2Ca$ phases at the grain boundaries and the interior of the grain, leading to preventing grain boundary sliding [8-10,16]. Another possible strengthening mechanism may be dispersion strengthening [17]. Jing [11] and Suzuki et al. [12] reported that Al_2Ca phases precipitate, and they improve the creep properties. Indeed, it is found that application of age hardening treatments to the Mg-Al-Ca alloys can improve the creep properties [12].

The addition of Mn in commercial Mg alloys is usually conducted so as to improve the corrosion resistance [18]. It is reported that the Mn addition can stimulate the formation of Al-Mn type particles which can sweep down iron, resulting in improving the purity in the melt. Nevertheless, it is found that the Mn addition can actually improve the creep property when the creep properties between the Mn-free and Mn-contianing Mg-Al-Ca alloys are compared.

In this study, creep properties in Mg-2Al-2Ca and Mg-2Al-2Ca-0.3Mn alloys were compared. The fine microstructures were analyzed by transmission electron microscopy (TEM) and atom probe tomography (APT).

Experimental procedures

Two types of alloys were investigated in this study. The alloy compositions are listed in Table 1 in mass and mol percent. In this investigation, Al, Ca and Mn are denoted as A, X and M, respectively, following the ASTM designation. Melting was conducted at 720 °C using Mg of 99.95% purity, and then Al and Al-10Mn master alloy were remelted by an electric furnace in a mixed-gas atmosphere of SF_6 and CO_2, and finally Ca was added to the melt. After stirring for about 1 min with the aid of Ar bubbling, the melt was poured into an iron mold held at 250-300 °C. The obtained cast dimensions were 150 × 120 × 40 mm. From the sample, creep test specimens and samples for microstructural observations were cut.

Table 1. Chemical composition (mass% and mol%).

Alloy	Element	Mg	Al	Ca	Mn
AX22	mass%	bal.	2.5	1.8	–
	mol%	bal.	2.3	1.1	
AXM220	mass%	bal.	2.2	2	0.3
	mol%	bal.	2.0	1.2	0.1

Flat specimens with a gauge length of 50 mm and reduced cross-sectional dimension of 10 × 5 mm were used for a tensile creep test using an A&D CP-6L-500 machine at temperature of 175 °C and an applied stress of 50 MPa. The temperature was maintained at ± 2 °C. No heat treatment was applied to the samples prior to the creep test.

The microstructures were observed using an Olympus BX60M optical microscope. Thin foils for the TEM observations were prepared by low energy beam ion thinning. Conventional TEM observations were made using a JEOL JEM-2010 microscope operated at 200 kV. The specimen thickness and structures of dispersed precipitates were measured using a convergent beam electron diffraction (CBED) technique, and the detailed methods can be found elsewhere [19].

Specimens for atom probe analyses were prepared by mechanical grinding and micro-electropolishing. These specimens were observed by a field ion microscope, and then analyzed by a locally built three dimensional atom probe (3DAP) equipped with a CAMECA fast delay line detector. Field evaporation was assisted by femtosecond laser pulses [20] with the following conditions; wavelength (UV: ultraviolet): 343 nm, pulse power: ~0.5 μJ/pulse; and pulse frequency 100 kHz. The measured temperature and vacuum conditions were 30 K and an ultrahigh vacuum of ~1×10^{-8} Pa, respectively.

Results and Discussion

Creep curves

Figure 1 shows creep curves obtained in the AX22 and AXM220 alloys crept at 175 ºC. The Mn-containing alloy shows a substantially improved (slow) creep rate. It is interesting to note that there was no report on the improved creep properties by the addition of Mn, although most of commercial Mg alloys contained Mn. The minimum creep rates ($\dot{\varepsilon}$) at 175 °C are 5.6×10^{-9} and 2.8×10^{-10} s^{-1} in the AX22 and AXM220 alloys, respectively. $\dot{\varepsilon}$ obtained in the AXM220 alloy is one order of magnitude lower

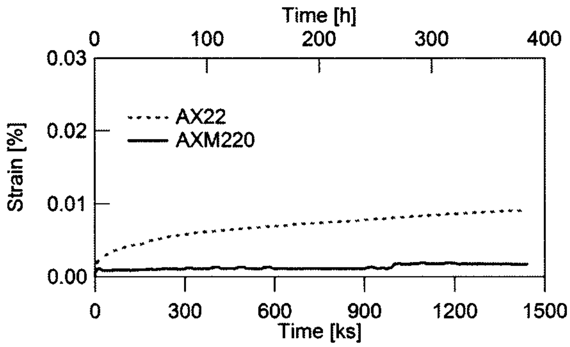

Figure 1. Creep curves obtained at 175 ºC and 50 MPa.

than that in the AX22 alloy. Thus, it is obvious that the Mn addition can improve the creep property of the Mg-Al-Ca system.

Grain boundary structures

Figure 2 indicates optical microscope images obtained in the as-cast samples. Coarse and network-shaped compounds appear at the grain boundaries and in the grains. The compounds were identified based on selected-area electron diffraction patterns, and it was found that the phases are mainly $(Mg,Al)_2Ca$. Mg_2Ca phases were also found. These results are well consistent with previous reports [8-11]. As the other authors reported, the compounds may prevent the grain boundary sliding during the creep deformation, resulting in improving the creep properties. Nevertheless, the Mn addition does not alter the morphology and structure of the compounds.

Intragranular precipitates in the as-cast samples

As shown in Fig. 2, some intragranular precipitates can be confirmed in the interior of the grains in both the alloys. The detailed morphology was observed using the TEM bright-field (BF) images as indicated in Fig. 3. The morphology of the precipitates is a plate shape, and the planar precipitates appear on the basal plane. This precipitate is consistent with Al_2Ca phase [11,12]. In contrast to results reported by Suzuki et al., our samples reveal the presence of the planar precipitate in the interior of the grains even after the as-cast state [12]. This may be due to the difference in the cooling rate between the permanent mold casting and die casting.

Based on foil thickness measurements using a CBED technique, the number densities of the planar precipitates were measured. The number densities of the AX22 and AXM220 alloys are 1.7×10^{19} and 1.8×10^{19} /m^3, respectively. Thus, the Mn addition does not influence the number density of the Al_2Ca phase in the as-cast conditions.

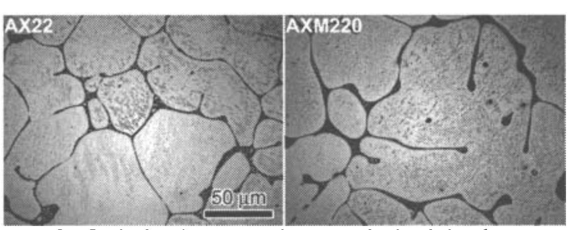

Figure 2. Optical microscope images obtained in the as-cast samples. The images are based on The 117th Conference of Japan Institute of Light Metals.

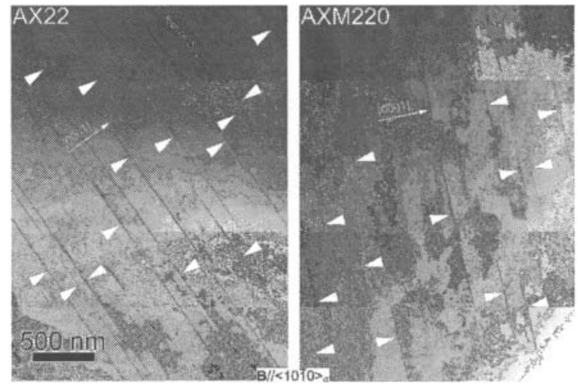

Figure 3. TEM BF images obtained in the as-cast samples. The white arrowheads indicate planar precipitates.

3DAP elemental maps of Al, Ca and Mn are obtained from the as-cast samples, and the results are given in Fig. 4. As can be seen in the Fig. 4, planar precipitates are detected. Based on the morphology, the planar precipitates are identified as the Al_2Ca phase. Note that the measured composition from the planar precipitates is lower than the stoichiometric composition of the Al_2Ca. This may be due to the fact that the compositional fluctuation may occur in the planar precipitates since the probe direction is parallel to the broad faces of the Al_2Ca phases: as a result, Mg concentration in the phases may be increased, resulting in lower concentration of Al, Ca and Mn. Although the concentration of the planar precipitates is low, CBED patterns reveal a C15 structure (a = 0.804 nm, space group $Fd\bar{3}m$ [21]). Hence, it is certain that the planar precipitates observed in the 3DAP elemental maps shown in Fig. 4 correspond to the Al_2Ca phase.

It should be noted that the partitioning behavior of Mn into the Al_2Ca phase is confirmed. However, the morphology and structure of the Al_2Ca as shown in Fig. 3 do not alter significantly. Segregation of Mn in the planar precipitates has been reported preciously [22]. This may affect the dislocation motion such as dislocation climb or dislocation glide. Hence, the Mn addition influences the creep property.

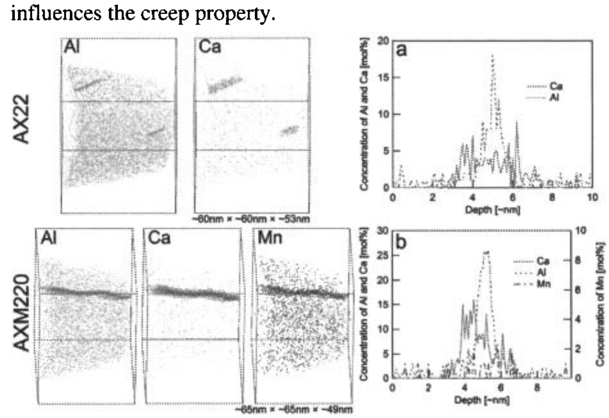

Figure 4. 3DAP elemental maps of Al, Ca or Mn in the as-cast specimens. (a) and (b) are concentration depth profiles obtained from the planar precipitates in the AX22 and AXM220 alloys, respectively.

Intraglanular precipitates in the crept specimens

Microstructures after the creep deformation were observed by conventional BF images, as indicated in Fig. 5. The specimens of the AX22 and AXM220 alloys were crept to the minimum creep rates, and the creep conditions were for 2051 h at 175 °C. The images were taken near $\boldsymbol{B} = [10\bar{1}0]_\alpha$ with three different g vectors ($\boldsymbol{g}$); i.e., $\boldsymbol{g} = \bar{2}112$, $\bar{2}110$ and 0002; Fig. 5 is obtained using $\boldsymbol{g} = \bar{2}110$. In both the alloys, the Al_2Ca phase precipitates on the basal plane of the matrix. The number densities were again measured based on the foil thickness measurement, and those in the AX22 and AXM220 alloys were 1.3×10^{19} and 1.9×10^{19} /m^3, respectively. Thus, the number densities before and after the creep test do not alter significantly at the minimum creep rate. In addition, the Mn addition does not influence the number density of the Al_2Ca phase in the crept specimens in spite of the partitioning behavior of Mn.

Despite the fact that the Al_2Ca phases do not influence the creep property in view of the number densities, some fine contrasts newly appear in the matrix between the planar Al_2Ca phases. These fine contrast can be seen when **g** is aligned to the $[\bar{2}110]$ direction. The coarse and planar precipitates are the Al_2Ca phase. As can be seen, small plate-like precipitates are observed with clear strain contrast as indicated by the white arrows. The plates are on the basal plane of the α-Mg matrix.

The measured number densities of the fine precipitates in the AX22 and AXM220 alloys are 4.4×10^{20} and more than 5.5×10^{20} /m^3, respectively. Since the fine precipitates observed in the AXM220 alloy is too small, some of them could not be counted. Hence, the number density in the AXM220 alloy is indeed underestimated. The average diameters of the fine precipitates along the direction perpendicular to $[0001]_\alpha$ are 19.4 and 14.3 nm in the AX22 and AXM220 alloys, respectively. Thus, the number density of the fine precipitates increases, while the diameter of the fine precipitates decreases by the Mn addition. In addition, it is found that the fine precipitates dynamically precipitate during the creep, regardless of the Mn addition.

Effect of fine precipitates on the creep property

The effect of dispersion strengthening on creep properties has widely been proposed [4-6, 23-27]. A continuous precipitation during creep test has been confirmed by TEM in a 2024PM (powder metallurgy) Al alloy [23]. The reported particle size is very small (~60 nm). They proposed that the dispersion strengthening may arise due to three different processes: (1) the bowing of dislocations between particles; (2) the back stress associated with the local climb of dislocations over particles; or

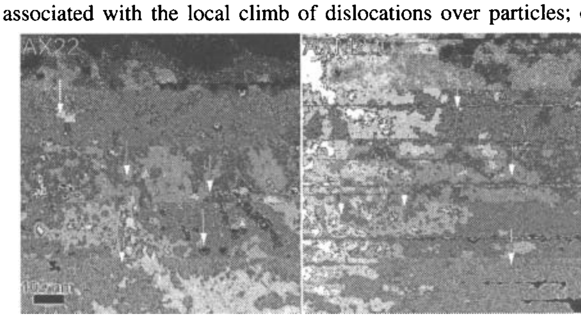

Figure 5. TEM BF images obtained in the crept specimens. The white arrows indicate fine and planar precipitates.

(3) the stress associated with detaching a dislocation from a particle. While Wang et al. [24] and Lumley et al. [25] reported the effect of dispersion of Ω phase in high temperature resistant Al-Cu-Mg-Ag alloys on the creep property. They found that the dispersion of the Ω phase can enhance the creep properties. By applying a T6 treatment before the creep test, the creep properties are improved [25].

A similar effect was reported by Suzuki et al. in an AXJ530 die cast alloy [12], although they applied the aging treatment without solution treatment. The creep properties are improved by dispersing the fine Al_2Ca phases before the creep test as they impede the nonbasal slip of the a-type dislocations during creep deformation.

The measured number density of the planar precipitates in both the crept AX22 and AXM220 alloys is, in fact, comparable to that peak aged Mg alloys [19,28,29]. The fine and planar precipitates observed in our alloys dynamically precipitate on the basal plane during the creep deformation. The Mn addition can further enhance the fine and dense precipitation. This may interfere the movement of the dislocations, leading to high creep resistance.

It should be emphasized that fine precipitations cannot be observed in the as-cast AXM220 alloy. This result is largely different from that reported preciously in an AXM6305 alloy [22]; fine and spherical Al-Mn precipitates appear in the as-cast state. It is reported that the enthalpy of mixing between Al and Mn is negatively large [30]. This means that aggregation or ordering of Al and Mn is the most stable state. Since the AXM220 alloy processes relatively low Al composition compared to the AXM6305 alloy, the formation of Al-Mn type precipitation may not easily occur; as a result, the precipitation behavior of the fine and planar precipitate is similar to the Mn-free alloy.

Conclusions

The effect of Mn addition on the creep property of the AX22 alloy has been investigated. The following conclusions were obtained. Coarse and network-shaped compounds form in the as-cast AX22 and AXM220 alloys. They may prevent the grain boundary sliding. The Mn addition does not influence the morphology and structure of the compounds. The planar Al_2Ca phase forms on the basal plane even in the as-cast samples. In the AXM220 alloy, Mn is detected in the Al_2Ca phase. This may cause strain fields around the phase, resulting in disturbing the dislocation motion. The number density of the Al_2Ca phase does not alter, regardless of the creep deformation and Mn addition. Fine and planar precipitates appear during the creep deformation. The number density is much higher in the AXM220 alloy than that in the AX22 alloy. The size of the precipitate is reduced by addition of Mn. The Mn addition can improve the creep property.

Acknowledgements

This work was supported in part by the Grant-in-Aid Scientific Research (A) 22246094, 2010. Mr. R. Asakawa of Nagaoka University of Technology, Japan is gratefully acknowledged for his support.

References

1. B.L. Mordike and W. Henning, "Creep and high temperature properties of magnesium based alloys," Magnesium Technology, The Inst. Met. London, (1987), 54-59.

2. H. Harimzadeh, et al., "Tensile and creep fracture of a Mg-Y-RE alloy," Magnesium Technology, (London, The Institute of Metals, 1987), 138-141.
3. M. Ahmed et al., "Creep fracture in a Mg-Y-RE alloy," Magnesium Alloys and Their Application, ed. B.L. Mordike and F. Hehmann (Oberursel, DGM Informationsgesellschaft m.b.H., 1992), 251-257.
4. M. Suzuki et al., "Creep behavior and deformation microstructures of Mg-Y alloys at 550 K," Materials Science and Engineering A, 252 (1998), 248-255.
5. I.A. Anyanwu et al., "Creep properties of Mg-Gd-Y-Zr alloys," Materials Transactions, 42 (2001), 1212-1218.
6. K. Maruyama, M. Suzuki and H. Sato, "Creep strength of magnesium-based alloys," Metallurgical and Materials Transactions A, 33A (2002), 875-882.
7. R. Ninomiya, T. Ojiro and K. Kubota, "Improved heat resistance of Mg-Al alloys by the Ca addition," Acta Metallurgica et Materialia, 43 (1995), 669-674.
8. A.A. Luo, M.P. Balogh and B.R. Powell, "Creep and microstructure of magnesium-alminum-calcium based alloys," Metallurgical and Materials Transactions A, 33A (2002), 567-574.
9. Y. Terada et al, "A thousandfold creep strengthening by Ca addition in die-cast AM50 magnesium alloy," Metallurgical and Materials Transactions A, 35A (2004), 3029-3032.
10. S.M. Zhu, B.L. Mordike and J.F. Nie, "Creep and rapture properties of a squeeze-cast Mg-Al-Ca alloy," Metallurgical and Materials Transactions A, 37A (2006), 1221-1229.
11. B. Jing et al., "Effect of extrusion on microstructures, and mechanical and creep properties of Mg-Al-Sr and Mg-Al-Sr-Ca alloys," Scripta Materialia, 55 (2006), 1163-1166.
12. A. Suzuki et al., "Precipitation strengthening of a Mg-Al-Ca-based AXJ530 die-cast alloy," Metallurgical and Materials Transactions A, 39A (2008), 696-702.
13. A. Luo and T. Shinoda, "Development of a creep-resistant magnesium alloy for die casting applications," Magnesium Alloys and their Applications, ed. B.L. Mordike and K.U. Kainer, (Frankfurt, Wekstoff-Informationsgesellschaft, 1998), 151-156.
14. F.v. Buch et al., "Development of a low-cost, temperature- and creep-resistant magnesium die-casting alloy," Magnesium Alloys and their Applications, ed. K.U. Kainer, (Darmstadt, WILEY-VCH, 2000), 23-28.
15. S. Koike et al., "Development of lightweight oil pans made of a heat-resistant magnesium alloy," HONDA R&D Technical Review, 12 (2000), 167-174.
16. A. Suzuki et al., "Structure and transition of eutectic $(Mg,Al)_2Ca$ Laves phase in a die-cast Mg-Al-Ca base alloy," Scripta Materialia, 51 (2004), 1005-1010.
17. M.E. Kassner, Fundamentals of Creep in Metals and Alloys (Oxford, Elsevier, 2009).
18. E.F. Emley, Principle of Magnesium Technology (New York, Pergamon Press, 1966).
19. T. Homma et al., "Effect of Zr addition on the mechanical properties of as-extruded Mg-Zn-Ca-Zr alloys," Materials Science and Engineering A, 527 (2010), 2356-2362.
20. T. Ohkubo et al., "Laser-assisted atom probe analysis of bulk insulating ceramics," MRS Proc. (2009), Fall Meeting.
21. P. Villars and L.D. Calvert, Pearson's Handbook of Crystallographic Data for Intermetallic Phases, second ed. (Materials Park, OH, ASM International, 1991).
22. T. Homma, S. Nakawaki and S. Kamado, "Improvement in creep property of a cast Mg-6Al-3Ca alloy by Mn addition," Scripta Materialia, (2010), in press.
23. L. Kloc et al., "Significance of continuous precipitation during creep of a powder metallurgy aluminum alloy," Materials Science and Engineering A, 216 (1996), 161-168.
24. J. Wang, X. Wu and K. Xia, "Creep behavior at elevated temperatures of an Al-Cu-Mg-Ag alloy," Materials Science and Engineering A, 234-236 (1997), 287-290.
25. R.N. Lumley, A.J. Morton and I.J. Polmear, "Enhanced creep performance in an Al-Cu-Mg-Ag alloy through underageing," Acta Materialia, 50 (2002), 3597-3608.
26. C.R. Hutchinson, P. Cornall and M. Goune , "On the origin of the enhanced creep resistance in underaged Al-Cu based alloys," Materials Science Forum, 519-521 (2006), 1029-1034.
27. C.K. Sudbrack et al., "Temporal evolution of the nanostructure and phase compositions in a model Ni-Al-Cr alloy," Acta Materialia, 54 (2006), 3199-3210.
28. C.L. Mendis et al., "Enhanced age hardening in a Mg-2.4at.%Zn alloy by trace additions of Ag and Ca," Scripta Materialia, 57 (2007) 485-488.
29. C.L. Mendis et al., "Precipitation-hardenable Mg-2.4Zn-0.1Ag-0.1Ca-0.16Zr (at.%) wrought magnesium alloy," Acta Materialia, 57 (2009), 749-760.
30. A.R. Miedema, F.R. de Boer and R. Boom, "Model predictions for the enthalpy of formation of transition metal alloys," CALPHAD, 1 (1977), 341-359.